

THERMOPHYSICAL PROPERTIES OF THE PHOENIX MARS LANDING SITE STUDY REGIONS.

N. E. Putzig¹, M. T. Mellon¹, M. P. Golombek², and R. E. Arvidson³. ¹Laboratory for Atmospheric and Space Physics, University of Colorado, Boulder, Colorado, USA. ²Jet Propulsion Laboratory, California Institute of Technology, Pasadena, California, USA. ³McDonnell Center for the Space Sciences, Department of Earth and Planetary Sciences, Washington University, St. Louis, Missouri, USA. Contact: Nathaniel.Putzig@Colorado.edu.

Introduction: The Phoenix Mars Mission, scheduled for launch in August 2007, will place a fixed lander on the northern polar plains to investigate the hydrologic history and search for evidence of habitability at the soil-ice boundary. In order to better constrain the characteristics of the landing site, we carried out an analysis of the thermophysical properties of five study regions in the annulus between 65°N and 72°N.

Maps of thermal inertia and albedo derived from three Mars years of Mars Global Surveyor (MGS) Thermal Emission Spectrometer (TES) data were used to evaluate the thermophysical properties of the study areas in a global context. As shown in Fig. 1, four of the five regions (A-D) have very similar intermediate albedo and thermal inertia and fall into duricrust-dominated Unit c first identified by Mellon et al. (2000) [1] and later refined by Putzig et al. (2005) [2]. Landing sites for the Mars Spirit Rover (MER-A) and both Viking Landers (VL-1 and VL-2) are also included in this unit. The fifth region (E) has higher thermal inertia and much lower albedo, placing it in Unit b, believed to be dominated by sand, rocks, and bedrock [1,2], which also includes the Mars Opportunity Rover (MER-B) landing site.

Background: Thermal inertia is the key material property controlling diurnal surface temperature and is defined as a combination of the bulk material properties of thermal conductivity k , density ρ , and heat capacity C such that $I \equiv (k\rho C)^{1/2}$. For typical geological materials under Mars surface conditions, conductivity generally dominates and is controlled primarily by physical properties, such as particle size, porosity, and pore connectivity, within the top few centimeters of the subsurface. Unconsolidated fines will have low values of thermal inertia, indurated dust and sand-sized particles will have intermediate values, and rocks and exposed bedrock will have high values. For observations made from orbit, the temperature of any given location on the surface is controlled by a variable mixture of such materials on the scale of the instrument resolution (~3 km for TES). To the extent that horizontal mixtures or near-surface layers of differing materials exist in the field of view, the thermal inertia derived from such temperature observations will vary with time of day

and season, due to the nonlinear relationship between temperature and thermal inertia [3,4].

Methodology: The global thermal inertia map used in Figs. 1 and 2, first presented by Putzig and Mellon (2005) [3], includes three Mars years of data from TES orbits 1583-24346. It was produced by taking the median value from 36 10°-L_s nightside thermal inertia maps binned at 1/2° per pixel (here, 'nightside' refers to the southbound leg of the MGS orbit, including periods when the Sun was above the horizon throughout the day at high latitudes). Albedo was mapped from TES visible bolometer data taken

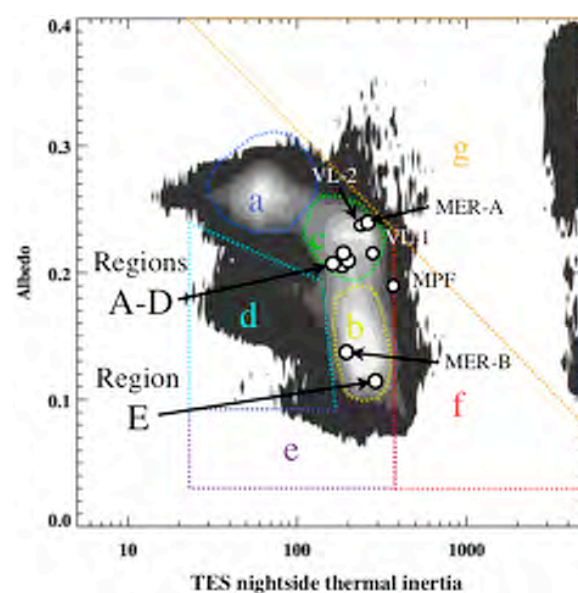


Figure 1. Global 2-dimensional histogram (filled contours) showing correlation between apparent thermal inertia (in $\text{J m}^{-2} \text{K}^{-1} \text{s}^{1/2}$) and albedo. Bin sizes are 0.012 in \log_{10} of thermal inertia and 0.010 in albedo. Circles show values for Phoenix Study Regions A-E and previous landing sites. Colored thermophysical unit boundaries a-g correspond to those in Figure 3.

over the same orbit range. Bounds for Units a-e in Fig. 1 are the same as those in Putzig et al. (2005) [2]. Units f and g were extended and modified to separate moderately high (f) from extremely high (g) thermal inertia values in the polar region, where the

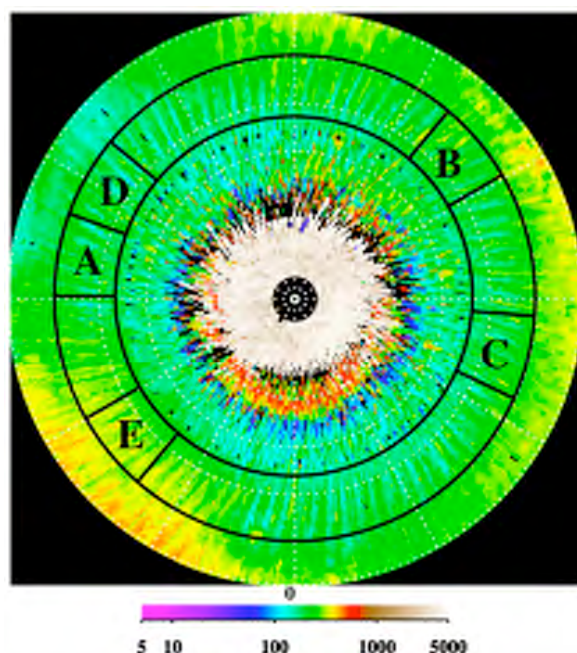


Figure 2. Nightside median apparent thermal inertia for the northern polar region (60-90°N), showing Phoenix Study Regions A-E in the 65-72°N annulus.

latter correspond predominantly to exposed water ice on the residual polar cap (orange in Fig. 3).

Results: Figure 2 shows the median annual thermal inertia for the region poleward of 60°N latitude. The orbit-track-aligned 'striping' is unlikely to represent true spatial variations but rather seasonal variations in derived thermal inertia made evident by systematic variations in coverage over the limited seasons ($\sim L_s=90-140$) of usable data at these latitudes. These apparent thermal inertia variations are probably due to widespread near-surface layering or sub-pixel horizontal mixing of materials in the polar region [3,4]. The mean values within each study region are quite similar for Regions A-D whereas Region E is about 75-100 $\text{J m}^{-2} \text{K}^{-1} \text{s}^{-1/2}$ higher. Correspondingly, the albedo values in Regions A-D are very comparable while that in Region E is much lower (Fig. 1). Remapping points in Fig. 1 to the surface (Fig. 3), we find that Regions A-D are broadly dominated by thermophysical Unit c, which has been interpreted as a duricrust unit [1,2], whereas Region E corresponds primarily to Unit b, interpreted as surfaces with a high percentage of sand, rocks, and/or bedrock [1,2].

The correspondence of study regions and past landing sites to specific thermophysical units suggests the possibility of extrapolating lander-

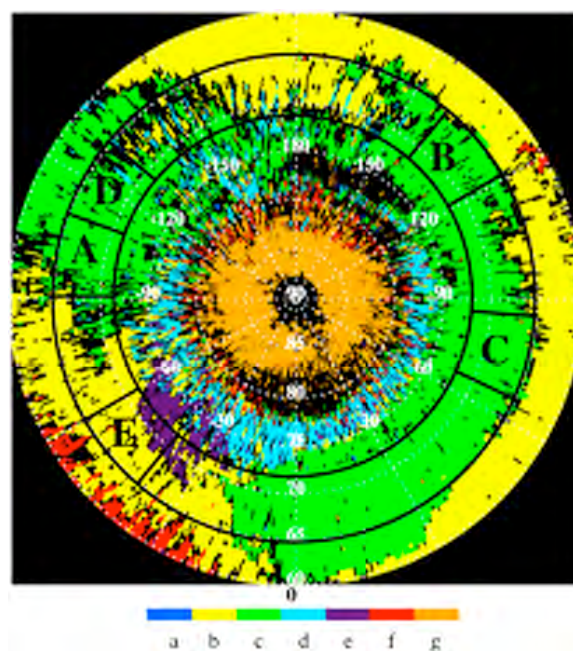


Figure 3. Thermophysical unit map of the northern polar region (60-90°N). Bounds of albedo and thermal inertia for Units a-g are shown in Fig. 1.

observed conditions to the study regions. Using thermal inertia values from Fig. 1 together with the observed VL-2 rock abundance of 18% and a relationship between thermal inertia and rock abundance from Fig. 16 of Golombek et al. (2003) [5], we obtain an estimate of 15-16% rock abundance in Region B. However, this extrapolation is somewhat suspect since thermal inertia may be affected by multiple processes and is generally not dominated by rock abundance [1,2]. Moreover, there is an increase in both thermal inertia and albedo between Region B and VL-2 whereas most physical processes which increase thermal inertia tend to reduce albedo (note the general global anti-correlation of these properties in Fig. 1). Additionally, if surface heterogeneity is dominating at one site and not at the other, or if different classes of heterogeneity are dominating at both sites, then any such extrapolation is likely to misrepresent the actual surface conditions.

References: [1] Mellon M. T. et al. (2000) *Icarus* 148. [2] Putzig et al. (2005) *Icarus* 173. [3] Putzig and Mellon (2005) *EOS Trans. AGU* 86 (52), Abstract P24A-02. [4] Putzig N. E. and Mellon M. T. (2006) *LPS XXXVII*. [5] Golombek et al. (2003) *JGR* 108 (E12).